

# Probing the Watson–Crick, Wobble, and Sugar-Edge Hydrogen Bond Sites of Uracil and Thymine

Andreas Müller, Jann A. Frey, and Samuel Leutwyler

Departement für Chemie und Biochemie, Universität Bern, Freiestrasse 3, CH-3012 Bern, Switzerland

Received: November 26, 2004; In Final Form: March 30, 2005

The nucleobases uracil (U) and thymine (T) offer three hydrogen-bonding sites for double H-bond formation via neighboring N–H and C=O groups, giving rise to the Watson–Crick, wobble and sugar-edge hydrogen bond isomers. We probe the hydrogen bond properties of all three sites by forming hydrogen bonded dimers of U, 1-methyluracil (1MU), 3-methyluracil (3MU), and T with 2-pyridone (2PY). The mass- and isomer-specific  $S_1 \leftarrow S_0$  vibronic spectra of 2PY·U, 2PY·3MU, 2PY·1MU, and 2PY·T were measured using UV laser resonant two-photon ionization (R2PI). The spectra of the Watson–Crick and wobble isomers of 2PY·1MU were separated using UV–UV spectral hole-burning. We identify the different isomers by combining three different diagnostic tools: (1) Selective methylation of the uracil N3–H group, which allows formation of the sugar-edge isomer only, and methylation of the N1–H group, which leads to formation of the Watson–Crick and wobble isomers. (2) The experimental  $S_1 \leftarrow S_0$  origins exhibit large spectral blue shifts relative to the 2PY monomer. Ab initio CIS calculations of the spectral shifts of the different hydrogen-bonded dimers show a linear correlation with experiment. This correlation allows us to identify the R2PI spectra of the weakly populated Watson–Crick and wobble isomers of both 2PY·U and 2PY·T. (3) PW91 density functional calculation of the ground-state binding and dissociation energies  $D_e$  and  $D_0$  are in agreement with the assignment of the dominant hydrogen bond isomers of 2PY·U, 2PY·3MU and 2PY·T as the sugar-edge form. For 2PY·U, 2PY·T and 2PY·1MU the measured wobble:Watson–Crick:sugar-edge isomer ratios are in good agreement with the calculated ratios, based on the ab initio dissociation energies and gas-phase statistical mechanics. The Watson–Crick and wobble isomers are thereby determined to be several kcal/mol less strongly bound than the sugar-edge isomers. The 36 observed intermolecular frequencies of the nine different H-bonded isomers give detailed insight into the intermolecular force field.

## I. Introduction

The structure of duplex DNA in aqueous solution is governed by a balance of noncovalent energies, e.g., stacking and hydrogen bond energies, as well as the constraints imposed by the molecular backbone, interaction with solvent water molecules and ions, thermal averaging and by collective vibrational modes. The interplay between these factors is complex and difficult to separate into specific contributions. To gain a detailed understanding of the individual contributions to the binding energy, it is necessary to remove the nucleobase pairs from their biological environment and study the pairwise interactions in the gas phase.<sup>1,2</sup>

The uracil and thymine dimers U·U and T·T can exist in eight different doubly H-bonded configurations, which have been previously studied by molecular mechanics and ab initio theoretical investigations.<sup>3–5</sup> Because 2-pyridone (2PY; see Figure 1) offers only *two* H-bonding groups compared to four in U and T, the number of different H-bonded isomers is restricted to three for the nucleobase dimer mimics 2-pyridone·uracil (2PY·U) and 2-pyridone·thymine (2PY·T) investigated in this work. Furthermore, because 2PY is sufficiently long-lived in the  $S_1$  excited state, these dimers are accessible to resonant two-photon ionization (R2PI) spectroscopy, whereas the dimers of uracil and thymine have extremely short excited-state lifetimes and exhibit broad, and unstructured R2PI spectra.<sup>6–8</sup>

We have recently investigated<sup>9</sup> 2PY·U, 2PY·T and 2-pyridone·5-fluorouracil (2PY·5FU) as mimics for the (uracil)<sub>2</sub>,

uracil·thymine and uracil·5-fluorouracil nucleic acid base pairs that occur in natural or synthetic RNA.<sup>10–13</sup> We have found that they bind via the N1–H donor group of U, T or 5FU, forming the so-called sugar-edge isomers,<sup>14</sup> shown in the top row of Figure 1. However, in DNA and RNA the N1–H groups of the pyrimidine nucleobases are glycosylated; hence, the sugar-edge isomers do not occur in the biological context. The biologically relevant Watson–Crick and wobble isomers are also connected by two neighboring N–H···O=C hydrogen bonds; see Figure 1. However, in the gas phase they have been calculated to be 3–5 kcal/mol less stable than the sugar-edge isomers.<sup>9</sup> In the crystal structure, the uracil molecules form centrosymmetric dimers with two N3–H···O=C4 hydrogen bonds,<sup>15</sup> as in the Watson–Crick dimer shown in Figure 1d.

In this work, we investigate the Watson–Crick, wobble and sugar-edge binding sites of uracil and thymine by forming doubly hydrogen-bonded complexes to 2-pyridone (Figure 1), using a combination of three diagnostic tools:

(1) Methylation studies employing 3-methyluracil (3MU), which can form only the sugar-edge complex with 2PY, as shown in Figure 1b, and 1-methyluracil (1MU), which can form both the Watson–Crick and wobble complexes, as shown in Figure 1d,e. For the latter, the isomers are separated by UV–UV hole-burning. Methylation studies on nucleobase pairs have previously been employed in molecular-beam studies on cytosine and adenine.<sup>16–18</sup>

(2) Comparison of the experimental and ab initio calculated spectral shifts of the  $S_1 \leftrightarrow S_0$  electronic origins. As we show

**TABLE 1: Ground-State Binding Energies  $D_e$ , Dissociation Energies  $D_0$ , Basis Set Superposition Errors BSSE, and Excited-State Dissociation Energies  $D_0(S_1)$  of the 2PY·3MU1, 2PY·1MU2, and 2PY·1MU3 Dimers Calculated at the PW91/6-311++G(d,p) Level<sup>a</sup>**

isomer	sugar edge			Watson–Crick			wobble		
	U1	T1	3MU1	U2	T2	1MU2	U3	T3	1MU3
$D_e(S_0)$	−20.7	−20.5	−20.5	−16.7	−16.4	−16.8	−15.3	−15.5	−15.0
BSSE	0.9	0.9	0.8	0.9	0.9	0.8	0.9	0.9	0.9
$D_0(S_0)$	−19.8	−19.6	−19.6	−15.8	−15.7	−16.2	−14.6	−14.8	−14.2
$D_0(S_1)^b$	−16.7	−16.6	−16.7	−13.7	−13.7	−14.1	−12.5	−12.7	−12.3
$\Delta G_{\text{isom}}^{\ominus}$	0.0 <sup>c</sup>	0.0 <sup>d</sup>		3.30 <sup>c</sup>	3.59 <sup>d</sup>	0.0 <sup>e</sup>	4.51 <sup>c</sup>	4.37 <sup>d</sup>	1.55 <sup>e</sup>

<sup>a</sup> The analogous values of the corresponding isomers<sup>9</sup> of 2PY·U and 2PY·T are given for comparison. <sup>b</sup> From  $D_0(S_0)$  and the experimental shift of the  $0_0^0$  transition. <sup>c</sup> Relative to U1,  $T = 513$  K. <sup>d</sup> Relative to T1,  $T = 483$  K. <sup>e</sup> Relative to 1MU2,  $T = 433$  K.

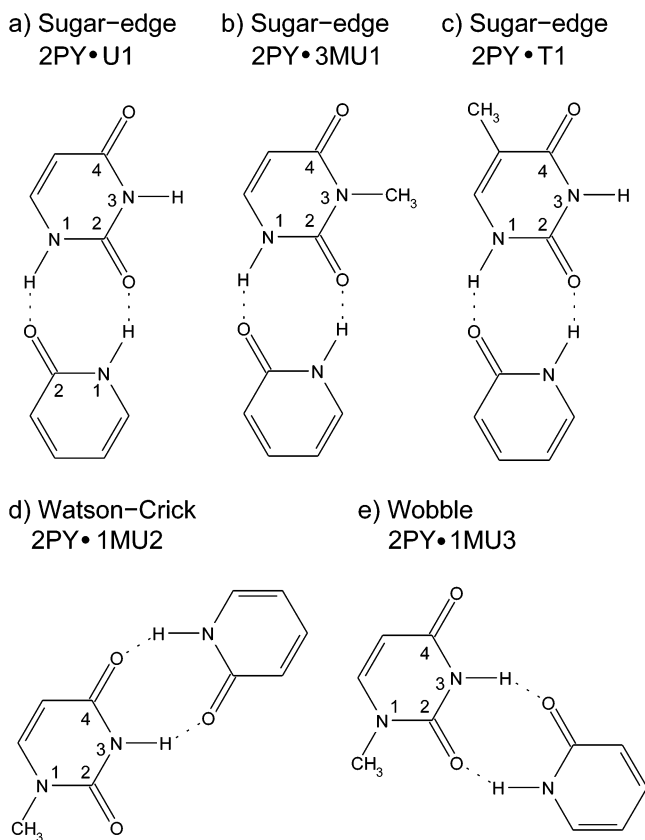


**Figure 1.** Structures of the sugar-edge dimers (a) 2-pyridone–uracil (2PY·U1), (b) 2-pyridone·3-methyluracil (2PY·3MU1), (c) 2-pyridone·thymine (2PY·T1), (d) the Watson–Crick (2PY·1MU2), and (e) wobble (2PY·1MU3) isomers of 2-pyridone-1-methyluracil. The sugar-edge, Watson–Crick, and wobble isomers are denoted by the suffixes 1–3, respectively.

below, CIS calculated spectral shifts correlate very well with the experimental shifts.

(3) PW91 density functional calculations of the dissociation energies  $D_0$  of the different hydrogen-bonded isomers.

All three diagnostic criteria are in full agreement with each other. On the basis of the comparisons, we are able to detect and confidently assign the Watson–Crick and wobble isomers of 2PY·U and 2PY·T, which are formed at the  $\approx 1\%$  level in the gas phase. These comparisons also prove the correctness of our previous assignment of 2PY·U and 2PY·T as the sugar-edge isomers.<sup>9</sup>

For all of these doubly hydrogen-bonded dimers, we observe that  $S_1 \leftarrow S_0$  electronic excitation of the 2-pyridone moiety decreases the intermolecular interaction strength by 2–3 kcal/mol, a  $\approx 15\%$  decrease of the total hydrogen bond dissociation energy. These decreases are explained and quantitatively

reproduced using excited-state configuration-interaction (CIS) ab initio calculations.

A total of 36 hydrogen bond vibrational frequencies of the sugar-edge, Watson–Crick and wobble isomers of 2PY·U, 2PY·T, 2PY·3MU and 2PY·1MU are determined in the  $S_1$  excited state. In combination with the CIS ab initio calculations, these reveal fundamental properties of the intermolecular force field around uracil and the methyluracils, free of other interactions.

The simultaneous observation of the Watson–Crick and wobble hydrogen bond isomers in the spectrum of 2PY·1MU, and of the sugar-edge, Watson–Crick and wobble isomers of 2PY·U and 2PY·T, allows us to determine the corresponding relative free energies of isomerization,  $\Delta G_{\text{isom}}^{\ominus}$ . These can be compared to the  $\Delta G_{\text{isom}}^{\ominus}$  values obtained from the density functional PW91 calculations combined with gas-phase statistical mechanics.

## II. Theoretical Methods and Results

Figure 1 shows the most stable hydrogen-bonded isomer structures of 2PY·U, 2PY·1MU, 2PY·3MU and 2PY·T (see also Table 1). These dimers involve two neighboring antiparallel N–H···O=C hydrogen bonds. There are analogous C–H···O=C hydrogen-bonded structures that are, however, much less strongly bound.<sup>3,19</sup> The  $\pi$ -stacked dimers are expected to be bound by  $D_e \approx -10$  kcal/mol, similar to the calculated stacking energy of (uracil)<sub>2</sub>.<sup>4,20</sup>

The minimum-energy structures, binding energies  $D_e$  and harmonic vibrational frequencies were calculated using the PW91 density functional and the 6-311++G(d,p) basis set for the electronic ground states. The doubly N–H···O=C hydrogen-bonded isomers of 2PY·U and 2PY·T have been previously investigated at the same level.<sup>9</sup> No symmetry restrictions were used and all isomers converged to planarity ( $C_s$  symmetry). The calculated binding energies  $D_e$  and dissociation energies  $D_0$  are compiled in Table 1. The basis set superposition errors (BSSE) are also listed for completeness.<sup>21,22</sup> Vibrational normal coordinate calculations were performed for all dimers. Table 1 also gives the free energies of isomerization  $\Delta G_{\text{isom}}^{\ominus}$  at the experimental temperatures of the molecular-beam nozzle for the three dimers 2PY·U, 2PY·1MU, and 2PY·T. These refer to the most stable isomer, i.e., the sugar-edge for 2PY·U and 2PY·T and the Watson–Crick isomer for 2PY·1MU. The isomerization thermodynamics are discussed in more detail in section IV.3. In the following, the suffixes 1–3 label the sugar-edge, Watson–Crick and wobble isomers, respectively.

3-Methyluracil can form only the sugar-edge isomer 3MU1; see Figure 1b. At the PW91 level, the 3MU1 isomer has a binding energy of  $D_e = -20.5$  kcal/mol and a dissociation energy  $D_0 = -19.6$  kcal/mol. The  $D_e$ 's and  $D_0$ 's of the sugar-edge isomer of 2PY·T (denoted T1) are identical and that of

**TABLE 2: Theoretical  $S_1$  State Vibrational Frequencies (in  $\text{cm}^{-1}$ ) Calculated for the 3MU, 1MU2, 1MU2, and the U1 and T1 Dimers, Calculated with the CIS Method Using the 6-31G(d,p) and 6-31(+G(d,p)) Basis Sets**

isomer	sugar edge			Watson–Crick			wobble		
	U1	T1	3MU1	U2	T2	1MU2	U3	T3	1MU3
CIS/6-31G(d,p)									
Intermolecular Vibrations									
buckle $\beta'$	19.1	17.4	18.8	19.4	18.8	17.2	18.5	16.6	18.1
propeller twist $\theta'$	43.9	41.6	39.5	36.5	32.9	33.1	36.2	35.6	35.8
stagger $\delta'$	61.3	59.4	59.5	63.7	62.0	58.0	63.5	57.6	61.4
opening $\omega'$	77.8	69.9	72.5	70.9	67.4	64.3	71.1	64.5	67.8
shearing $\chi'$	82.0	87.9	89.5	85.3	84.3	84.5	85.8	84.8	84.8
stretch $\sigma'$	128.5	126.4	122.8	124.6	112.4	123.1	121.3	120.2	110.8
Intramolecular Vibrations									
2PY butterfly def $\mu'$	90.0	79.7	78.4	79.9	79.6	76.0	80.8	78.5	80.2
uracil oop $\text{CH}_3$ torsion $\tau'$		165.4	83.3		170.2	78.2		169.92	75.4
CIS/6-31(+G(d,p))									
Intermolecular Vibrations									
buckle $\beta'$	19.3	17.5	19.1	17.2	18.9	17.6	19.7	17.0	19.0
propeller twist $\theta'$	46.8	44.3	42.1	39.8	35.8	39.4	39.5	38.3	35.4
stagger $\delta'$	66.9	64.9	64.4	67.9	64.7	70.2	67.8	61.3	74.5
opening $\omega'$	81.3	72.9	75.6	71.7	75.3	62.9	72.0	69.0	64.1
shearing $\chi'$	89.0	87.5	89.8	86.2	86.5	86.5	85.4	84.7	85.5
stretch $\sigma'$	131.6	131.6 <sup>a</sup>	125.7	126.4	115.5	128.8 <sup>a</sup>	123.1	121.9 <sup>a</sup>	115.1 <sup>a</sup>
Intramolecular Vibrations									
$\text{CH}_3$ torsion $\tau'$		164.9	84.7		174.6	77.2		170.0	78.1
uracil oop deformation		126.4			118.7	124.3		126.4	113.7
2PY butterfly def $\mu'$	166.4	167.8	166.0	164.1	165.0	165.7	164.6	164.3	164.6

<sup>a</sup> Coupling of  $\sigma$  with a uracil out-of-plane ring deformation.

2PY·U (denoted U1) is 0.2 kcal/mol larger, showing that methylation has only a small influence on the hydrogen bond interaction. 1-Methyluracil can form the Watson–Crick isomer labeled 1MU2; cf. Figure 1d. Its PW91 calculated  $D_e$  is  $-16.8$  kcal/mol, which is 0.1 and 0.3 kcal/mol larger than those calculated for the 2PY·U and 2PY·T Watson–Crick dimers U2 and T2. On the other hand, formation of H-bonds via N3–H and C2=O gives the so-called wobble dimer 1MU3; see Figure 1e. Its PW91 calculated  $D_e$  is  $-15.0$  kcal/mol, respectively, which is 0.3 and 0.5 kcal/mol smaller than those calculated for the 2PY·U and 2PY·T dimers U3 and T3.

In summary, the sugar-edge dimers are about 4 kcal/mol more stable than the Watson–Crick dimers and these in turn are 1–2 kcal/mol more stable than the wobble dimers. The influence of methylation of uracil at the N1-, N3-, and C5 positions on the hydrogen bond dissociation energies is small, in the range of  $\pm 0.3$  kcal/mol.

**Excited-State Calculations.** Full structure optimizations for the  $S_1$  states were performed for all dimers and isomers using the CIS method with the 6-31G(d,p) and 6-31(+G(d,p)) basis sets. The latter basis set includes diffuse functions on both donor hydrogen atoms.<sup>23–25</sup> These yielded slightly nonplanar structures ( $C_1$ ), in which the 2-pyridone moiety is pyramidalized at the N–H group, the N–H orientation being equatorial.<sup>9,26,27</sup> The propensity to out-of-plane deformation is also reflected in the low-frequency out-of-plane 2PY ring deformation mode  $\mu'$ , which is calculated to lie at  $\approx 80$   $\text{cm}^{-1}$  with the 6-31G(d,p) basis set and at  $\approx 165$   $\text{cm}^{-1}$  with the 6-31(+G(d,p)) basis; see Table 2. The calculated inversion barriers to inversion at the N atom are very low, 0.03 kcal/mol for 3MU and 1MU2 and 0.02 kcal/mol for 1MU3.

### III. Experimental Method and Results

**A. Methods.** The 2-pyridone·methyluracil dimers were synthesized and cooled in a 20 Hz pulsed supersonic expansion through a thin-walled 0.6 mm diameter orifice, using Ne carrier

gas at a backing pressure of 0.8–1.4 bar. 2-Pyridone (Aldrich, 97%) was placed in a heated (90 °C) stainless steel container through which the Ne carrier gas was flowed; the connection tube between the bubbler and the nozzle was held at 100 °C. 1-Methyluracil (Aldrich, 99%) or 3-methyluracil (RI Chemical, 99%) were placed in the pulsed nozzle, which was heated to 160 °C for 1MU, 180 °C for 3MU, 185 °C for thymine, and 215 °C for uracil.<sup>9</sup>

Mass-selected two-color resonant two-photon ionization (2C–R2PI) spectra were measured in the region 30 000–32 500  $\text{cm}^{-1}$  by crossing the skimmed supersonic jet with the unfocused UV excitation and ionization laser beams brought to spatial and temporal ( $\pm 0.5$  ns) overlap in the source of a linear time-of-flight mass spectrometer.  $S_1 \leftarrow S_0$  excitation was performed by a frequency-doubled dye laser at pulse energies of 0.2–1 mJ, pumped by the second harmonic of a Nd:YAG laser. For ionization the fourth harmonic (266 nm) of the same Nd:YAG laser was used at energies of 1–2 mJ/pulse. The ions were detected using double multichannel plates. The resulting mass spectra were digitized in a LeCroy LT374 digitizer, averaged over 64 laser shots and transferred to a PC.

UV–UV hole-burning experiments were performed using a second frequency-doubled dye laser pumped by a different frequency doubled Nd:YAG laser (Continuum Surelite II). The pulse energies for hole-burning were 1–2 mJ/pulse. The temporal delay between the hole-burning and the probe lasers was  $\approx 100$  ns.

**B. 2-Pyridone·3-Methyluracil.** The lowest  $\approx 700$   $\text{cm}^{-1}$  of the two-color R2PI spectrum of 2PY·3-methyluracil are shown in Figure 2. The low-frequency intense band at 30 866.9  $\text{cm}^{-1}$  is assigned as the  $S_1 \leftarrow S_0$  origin of the 2PY moiety in the dimer. The intense bands at 530.7 and 556.9  $\text{cm}^{-1}$  are assigned to the  $\nu'_5$  and  $\nu'_6$  in-plane ring deformation vibrations of 2PY. The overall structure is quite similar to the 2C–R2PI spectrum of 2PY·thymine,<sup>9</sup> which is shown in Figure 2b for comparison. The R2PI spectrum can be observed up to an excess energy of

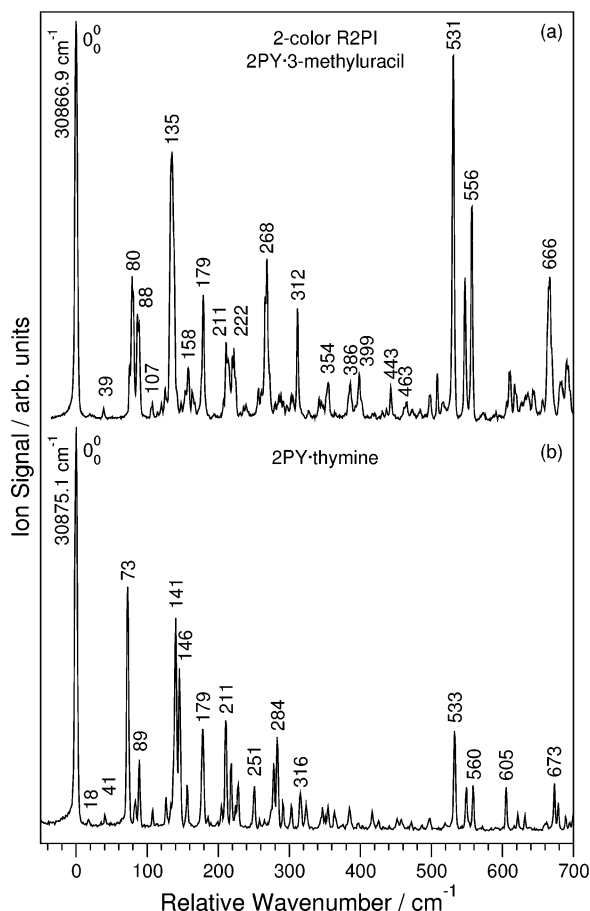


**Figure 2.** Two-color resonant two-photon ionization spectra of (a) 2-pyridone·3-methyluracil and (b) 2-pyridone·thymine. The wavenumber scales are relative to the electronic origins at (a) 30 866.9  $\text{cm}^{-1}$  and (b) 30 875.1  $\text{cm}^{-1}$ .

$\approx 1500 \text{ cm}^{-1}$ . UV–UV hole-burning measurements at the electronic origin show that the entire spectrum is due to a single isomer.

Given the calculated planarity of the dimer in the  $S_0$  state, near-planarity in the  $S_1$  state, and the in-plane orientation of the  $S_1 \leftrightarrow S_0$  electronic transition in the 2-pyridone moiety,<sup>28</sup> we expect the in-plane intermolecular vibrations ( $a'$  in  $C_s$ ) to dominate the spectrum. We assign the excitation at 80  $\text{cm}^{-1}$  to the opening fundamental  $\omega'$ , predicted at 72.5  $\text{cm}^{-1}$  by the CIS/6-31G(d,p) calculation. The slightly weaker band at 88  $\text{cm}^{-1}$  is assigned to the shearing mode  $\chi'$ , calculated at 89.5  $\text{cm}^{-1}$ . The intense band at 135  $\text{cm}^{-1}$  corresponds to the  $\sigma'$  hydrogen bond stretch, calculated at 122.8  $\text{cm}^{-1}$ . A progression in this mode is observed up to  $3\sigma'$  at 399  $\text{cm}^{-1}$ . Many further combination and overtone bands are assigned in Table 3.

The weak transition at 39.0  $\text{cm}^{-1}$  is assigned to the propeller twist  $\theta'$  fundamental. The weak band at 125.3  $\text{cm}^{-1}$  is assigned as the overtone of the stagger vibration  $2\delta'$ , in analogy to the spectra of 2PY·T Figure 2b and of 2PY·U in ref 9. The resulting fundamental frequency of 62.7  $\text{cm}^{-1}$  is in good agreement with the CIS calculations.

At 178.9  $\text{cm}^{-1}$  a medium strong band is observed that cannot be an intermolecular fundamental, because its frequency is higher than that of the H-bond stretch. On the other hand, its intensity is too high for it to be a combination or overtone. Built on this state are combinations with the intermolecular vibrations  $\omega'$  at 257 and  $\sigma'$  at 312  $\text{cm}^{-1}$ . We have previously observed analogous bands in the  $S_1 \leftarrow S_0$  spectra of 2PY·U, 2PY·T and 2PY·5FU at 178.2, 178.4 and 177.0  $\text{cm}^{-1}$ , respectively.<sup>9</sup> We

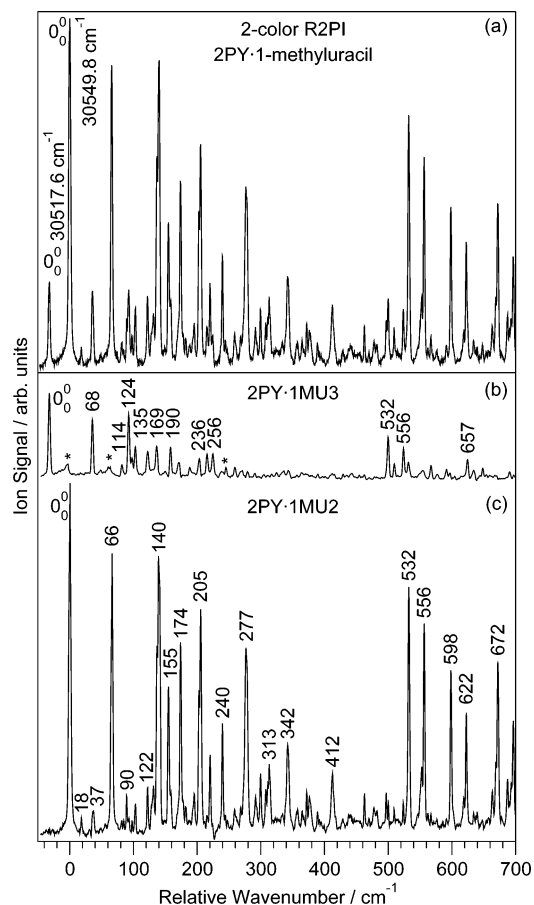


**Figure 3.** (a) Two-color R2PI spectrum of 2-pyridone·1-methyluracil. (b) UV–UV hole-burning difference spectra of the wobble isomer 1MU3 and (c) of the Watson–Crick isomer 1MU2. The wavenumber scale is relative to the  $0_0^0$  band of the 1MU2 isomer at 30 517.6  $\text{cm}^{-1}$ . The residuals from the subtraction procedure are marked by  $\star$ .

tentatively assigned these excitations in terms of the “B” origin, which lies 95  $\text{cm}^{-1}$  above the A origin in bare 2PY.<sup>28,29</sup> The B origin has been interpreted as being due to a nonplanar excited-state conformer with a pseudoaxial orientation of the N–H bond.<sup>28</sup> We speculate that this conformer origin is shifted from +95 to about +178  $\text{cm}^{-1}$  by the double hydrogen bond formation in these dimers.

**C. 2-Pyridone·1-Methyluracil.** The two-color R2PI spectrum of 2PY·1MU is shown in Figure 3a. At the low-frequency end, a band of medium intensity is observed at 30 517.6  $\text{cm}^{-1}$ , followed by a 5 times stronger band 32.2  $\text{cm}^{-1}$  to the blue. UV–UV hole-burning spectra taken with the detection laser on either band show these to be due to different isomers: The isomer selected spectra obtained by UV–UV hole-burning and subtraction are shown in Figure 3b,c, respectively. We attribute the more abundant isomer to the Watson–Crick isomer 1MU2 and the other to the wobble isomer 1MU3, cf. Figure 1d,e; see also the discussion below. The band positions and assignments are compiled in Table 3.

In the R2PI spectrum of the Watson–Crick isomer, Figure 3c, the weak band at 18  $\text{cm}^{-1}$  is assigned to the buckle vibration  $\beta'$ , on the basis of the CIS/6-31G(d,p) frequency of 17.2  $\text{cm}^{-1}$  and its weakness, appropriate for an out-of-plane fundamental. An analogous  $\beta'$  excitation is clearly observed at 18  $\text{cm}^{-1}$  in the spectrum of 2PY·thymine,<sup>9</sup> see Figure 2b. The weak band at 37  $\text{cm}^{-1}$  is assigned to the propeller twist  $\theta'$ . The frequency is in good agreement with the CIS/6-31G(d,p) value of 33.1  $\text{cm}^{-1}$ , and its intensity is similar to that of the  $\theta'$  bands of 2PY·3MU at 39  $\text{cm}^{-1}$  and of 2PY·T at 41  $\text{cm}^{-1}$ .

**TABLE 3: Experimental  $S_1$  State Vibrational Frequencies (in  $\text{cm}^{-1}$ ) of 2-Pyridone-3-Methyluracil, 2-Pyridone-1-Methyluracil Isomers 1MU2 and 1MU3, 2-Pyridone-Uracil, and 2-Pyridone-Thymine**

	2-pyridone-3-methyluracil	2-pyridone-1-methyluracil		2-pyridone-uracil	2-pyridone-thymine
	3MU	1MU2	1MU3	U1	T1
$\beta'$		18.2			17.6
$\theta'$	39.0	36.8		45.0	40.9
$\omega'$	79.7	65.5	67.6	82.2	72.6
$2\theta'$	75.4				83.3
$\chi'$	87.6	89.8	80.8	86.2	89.0
$\theta' + \delta'$	107.1			110.4	107.7
$\omega' + \theta'$	120.5	102.4			
$2\delta'$	125.3	122.1	114.1	129.3	126.8
$\sigma'$	134.7	139.5	124.1	141.7	140.1
$\omega' + 2\theta'$	153.4			157.5	156.5
$2\omega'$	157.9	130.7	134.5	164.4	145.5
$\omega' + \chi'$	163.5	154.7	154.1		
$B$	178.9	173.7	169.1	178.2	178.4
$\omega' + \sigma'$	211.3	204.9	190.4	222.4	210.8
$\chi' + \sigma'$	222.0	220.0	203.4	227.9	228.1
$3\omega'$	235.9	194.6		245.0	218.3
$B + \omega'$	256.5	239.8	235.6	258.5	250.8
$B + \chi'$	266.3			261.0	265.5
$2\sigma'$	268.4	276.8	246.8	281.0	278.3
$2\omega' + \sigma'$	286.9	269.3	255.8	303.7	283.2
$2\chi' + \sigma'$	303.9				
$B + \sigma'$	311.9	312.6	291.4	316.6	315.8
$4\omega'$				323.9	291.4
$B + 2\omega'$	327.7	299.1	302.2		324.0
$\omega' + 2\sigma'$	341.7	342.1	311.5	360.3	347.3
$2B$	354.3				
$\chi' + 2\sigma'$				367.0	364.4
$3\omega' + \sigma'$				385.2	354.8
$B + \omega' + \sigma'$	385.5	376.9	357.2		
$3\sigma'$	398.5	412.0	367.5	417.0	417.2
$4\omega' + \sigma'$					425.4
$B + 2\sigma'$	442.9				
	463.4	462.8			
					497.8
$\omega' + 3\sigma'$	472.8	477.6		496.8	
$\chi' + 3\sigma'$	483.9	500.2			
$4\sigma'$		552.5			
$\nu'_5(2PY)$	530.7	532.1	532.3	533.8	532.7
	547.4		542.0		
$\nu'_6(2PY)$	556.9	556.1	555.5	556.7	549.5
$B + 3\sigma'$	572.8		564.2		
$\nu'_5(2PY) + \omega'$	610.4	598.2	599.0	616.1	605.3
$\nu'_5(2PY) + \chi'$		618.6			
$\nu'_6(2PY) + \omega'$		621.9	622.5		
$\nu'_6(2PY) + \chi'$		639.7			
$\nu'_5(2PY) + \sigma'$	665.9	671.7	656.9	674.5	673.3
$\nu'_6(2PY) + \sigma'$		695.8	679.0		

The intense band at  $66 \text{ cm}^{-1}$  is assigned to the opening  $\omega'$  mode; the CIS/6-31G(d,p) frequency is  $64.3 \text{ cm}^{-1}$ , in good agreement. This is the lowest  $\omega'$  frequency observed for any of the methyluracil dimers. In contrast to the 2PY-3MU spectrum, the shear vibration  $\chi'$  at  $89.8 \text{ cm}^{-1}$  is very weak. The  $\omega' + \chi'$  combination band is observed at  $154.7 \text{ cm}^{-1}$ ; it is unusually intense due to Fermi resonance with the  $\sigma'$  stretch level (see below). The weak band at  $122 \text{ cm}^{-1}$  is assigned to the  $2\delta'$  stagger overtone, as for 2PY-3MU. The strongest R2PI band at  $140 \text{ cm}^{-1}$  is assigned to the  $\sigma'$  fundamental. Here, the stretch progression is observable up to  $4\sigma'$  at  $553 \text{ cm}^{-1}$ . The medium strong band at  $174 \text{ cm}^{-1}$  is assigned as the 2PY B electronic origin, as discussed above for 2PY-3MU. It combines with the same fundamentals as the  $0_0^0$  origin transition. The intense bands at  $532$  and at  $556 \text{ cm}^{-1}$  are assigned to the  $\nu'_5(2PY)$  and  $\nu'_6(2PY)$  intramolecular vibrations of 2PY, which also carry intense combinations with intermolecular excitations.

In the less intense R2PI spectrum of the wobble isomer 1MU3, Figure 3b, the features at  $32$  and at  $95 \text{ cm}^{-1}$  are artifacts from subtraction of the two hole-burning spectra due to slight differences of the intensities of the band wings. At  $68 \text{ cm}^{-1}$  the intense  $\omega'$  opening vibration is observed. The  $\chi'$  fundamental is tentatively assigned to the very weak feature at  $81 \text{ cm}^{-1}$ , but it may also be hidden under the  $95 \text{ cm}^{-1}$  subtraction artifact. The intense band at  $124 \text{ cm}^{-1}$  is assigned to the  $\sigma'$  stretch fundamental: this frequency is between  $11$  and  $16 \text{ cm}^{-1}$  lower than for the other isomer and the other methyluracils investigated. The overtones are observed at  $2\sigma' = 246.8 \text{ cm}^{-1}$  and  $3\sigma' = 367.5 \text{ cm}^{-1}$ . The 2PY B origin is observed at  $169.1 \text{ cm}^{-1}$ , slightly lower than in the other spectra. The combination bands  $B + \omega'$  at  $235.6 \text{ cm}^{-1}$ ,  $B + \sigma'$  at  $291.4 \text{ cm}^{-1}$  and higher combinations are also observed. The strong bands at  $532$  and at  $556 \text{ cm}^{-1}$  are assigned to the  $\nu'_5(2PY)$  and  $\nu'_6(2PY)$  intramolecular vibrations of 2PY.

#### IV. Discussion

**A. Assignment of the 2PY·1-Methyluracil Isomers.** The assignments of the spectra in Figure 3b,c as due to the wobble (1MU3) and Watson–Crick (1MU2) isomers, respectively, are based on the comparisons of the experimental vibrational frequencies and frequency differences with the CIS/6-31G(d,p) calculated ones: The  $\omega'$  frequency of 1MU2 is 65.5 or 2.1  $\text{cm}^{-1}$  smaller than that of 1MU3. On the other hand, the intermolecular stretch frequency of 1MU2 is  $\sigma' = 139.5 \text{ cm}^{-1}$ , which is 15.4  $\text{cm}^{-1}$  larger than that of 1MU3. The observed signs and magnitudes of both vibrational frequency differences are in good agreement with the CIS calculations with both the 6-31G(d,p) and 6-31(+)-G(d,p) basis sets; cf. Table 2.

Furthermore, the ground-state PW91 calculation predicts the dissociation energy of the Watson–Crick isomer (1MU2) to be 2.0 kcal/mol larger than that of the wobble isomer (1MU3). These relative energies are in agreement with the previous assignment based on vibrational frequencies. The observed Watson–Crick:wobble isomer ratio can be shown to be in quantitative agreement with calculation if we assume that the equilibration occurs within the molecular-beam source and that the subsequent supersonic expansion simply freezes out this ratio. The  $S_1 \leftarrow S_0$  electronic transition is localized within the 2PY moiety, and we assume that the oscillator strengths are identical for both isomers. Then, the relative intensities of the 1MU2 and 1MU3 spectra directly reflect the population ratio of the isomers. The isomer equilibrium ratio in the molecular-beam source can be calculated from the free energy change of the isomerization  $1\text{MU2} \rightarrow 1\text{MU3}$  at the source temperature  $T = 433 \text{ K}$ . At the PW91/6-311++G(d,p) level and using the harmonic-oscillator/rigid rotor approximation, the calculated free energy of isomerization is  $\Delta G_{\text{isom}}^0 = +1.61 \text{ kcal/mol}$  (Table 1). This converts to a 1MU2:1MU3 ratio of 6.5:1 at  $T = 433 \text{ K}$ , very close to the observed ratio of 4:1. We conclude that the Watson–Crick:wobble isomer ratio is established within the molecular-beam source and/or very early in the expansion.

If the supersonic cooling in the expansion far downstream of the nozzle modifies the isomer ratio, it will favor the lower-energy isomer, i.e., increase the isomer ratio beyond that calculated, which is in contrast to observation. Furthermore, the most probable interconversion path of the wobble  $\rightarrow$  Watson–Crick isomerization involves dissociation of the (2PY)-N–H $\cdots$ O=C2 hydrogen bond, followed by relative rotation of the 2PY and 1MU moieties around the remaining (2PY)-C=O $\cdots$ H–N3 hydrogen bond. The barrier for this process is  $\approx 8 \text{ kcal/mol}$ , and the masses involved in the relative rotation are large. We expect this isomerization rate to be insignificant relative to the very rapid cooling in the supersonic jet.

**B. Experimental and Calculated Spectral Shifts.** The  $S_1 \leftarrow S_0$  electronic origins of 2PY complexed to uracil and the methyluracils are shifted to the blue of the electronic origins of 2PY. We will refer all spectral shifts to the *A* origin<sup>28,29</sup> of 2PY at 29 831.3  $\text{cm}^{-1}$ . The spectral shift reflects the change of the H-bond dissociation energies upon electronic excitation,  $\delta\nu = D_0(S_1) - D_0(S_0)$ ; a blue shift corresponds to a lowering of  $D_0$ . For 2PY·U,<sup>9</sup> 2PY·T<sup>9</sup> and 2PY·3MU, the shifts are  $\delta\nu = +1080.3$ ,  $+1043.2$  and  $+1035.6 \text{ cm}^{-1}$ , respectively, corresponding to decreases of 3.0–3.3 kcal/mol. The 2PY·1MU isomers exhibit considerably smaller shifts,  $\delta\nu(1\text{MU2}) = +718.5 \text{ cm}^{-1}$  and  $\delta\nu(1\text{MU3}) = +686.3 \text{ cm}^{-1}$ , corresponding to decreases of 2.05 and 1.96 kcal/mol.

Spectral blue shifts in the 500–1000  $\text{cm}^{-1}$  range have been observed for other doubly hydrogen-bonded complexes of 2-pyridone, e.g., the self-dimer (2PY)<sub>2</sub>,<sup>26,27,30,31</sup> the tautomer

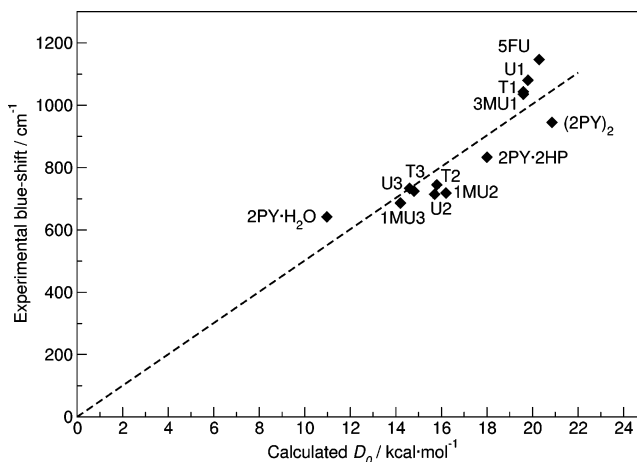


**Figure 4.** Correlation of experimental spectral blue shifts of the 2-pyridone·X dimers vs the PW91/6-311++G(d,p) calculated dissociation energy  $D_0(S_0)$ , where X = 5-fluorouracil (5FU), uracil, thymine, 3-methyluracil, 2-pyridone, 2-hydroxypyridine (2HP), 1-methyluracil, H<sub>2</sub>O. The sugar-edge, Watson–Crick and wobble isomers are labeled by the suffixes 1–3, respectively. The value for H<sub>2</sub>O is from ref 33.

dimer 2PY·2-hydroxypyridine,<sup>32,33</sup> and the mono- and dihydrate clusters 2PY·H<sub>2</sub>O and 2PY·(H<sub>2</sub>O)<sub>2</sub>.<sup>34</sup> In hydrogen-bonding solvents,  $\pi\pi^*$  transitions typically shift to lower-frequency upon H-bond formation, whereas  $n\pi^*$  transitions shift to the blue.<sup>35</sup> Very large spectral blue shifts upon solvation are typical for transitions to Rydberg states, due to repulsion of the diffuse orbitals by the surrounding solvent. We have previously suggested that the spectral blue shifts of the  $S_1 \leftrightarrow S_0$  transitions of 2PY may be due to mixing of  $\pi\pi^*$  with low-lying Rydberg-type  $\pi\sigma^*$  excitations.<sup>9</sup> The role of low-lying  $\pi\sigma^*$  excitations for the excited-state photophysics and photochemistry of phenol, indole and other heteroaromatics has been pointed out by Domcke and co-workers.<sup>36,37</sup>

In Figure 4 we plot the observed spectral shifts  $\delta\nu$  vs the PW91 calculated ground-state dissociation energies  $D_0(S_0)$ . In the limit of no interaction,  $\delta\nu$  must be zero; we have included this as a condition for the dashed line drawn in Figure 4. The spectral shift is seen to correlate quite well with  $D_0(S_0)$ : The decrease of dissociation energy upon electronic excitation is roughly 15% of the ground-state dissociation energy. The excited-state  $D_0(S_1)$  values, calculated from the PW91  $D_0(S_0)$  values and the experimental blue shifts are also given in Table 1.

Using the SCF and CIS methods for the  $S_0$  and  $S_1$  states, we calculated the adiabatic  $S_1 \leftarrow S_0$  transition energies for the dimers of 2PY with uracil, 1MU, 3MU, T (5MU), 5-fluorouracil (5FU), and 2-hydroxypyridine and H<sub>2</sub>O. As expected for CIS calculations, the absolute transition energies are too high, in this case by about 40%. However, the calculated spectral shifts correlate very well with the experimental shifts, as shown in Figure 5. The regression coefficient is  $r = 0.996$  if the linear correlation is also required to pass through the origin. The calculated slope is 1.279; i.e., the calculated shifts are about 22% smaller than the experimental ones. In Figure 5 we also show the spectral shifts calculated with the 6-31(+)-G(d,p) basis set, which contains diffuse orbitals on the H atoms of the N–H or O–H groups involved in hydrogen bonding. The correlation between calculated and observed shifts is much less good,  $r = 0.6911$ . We note that the two outliers are 2PY·2-hydroxypyridine and 2PY·H<sub>2</sub>O, which have hydrogen bonds that are qualitatively different from the nine other complexes. The calculated shifts are 33% smaller than the experimental ones.

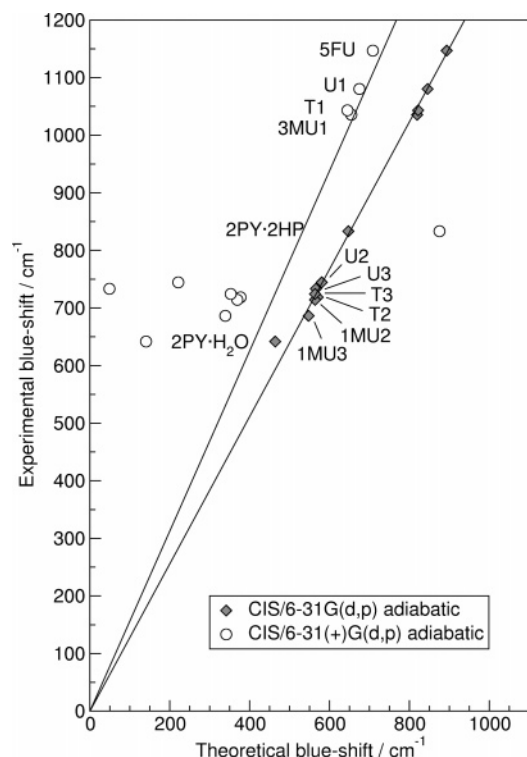


**Figure 5.** Experimental spectral shifts of the 2PY·X dimers vs the CIS calculated adiabatic spectral shifts, where X = 5-fluorouracil, uracil, thymine, 3-methyluracil, 2-hydroxypyridine, 1-methyluracil and H<sub>2</sub>O. The value for H<sub>2</sub>O is from ref 33. The theoretical spectral shifts are calculated using the 6-31G(d,p) and the 6-31(+G(d,p)) basis sets.

The SCF and CIS/6-31G(d,p) calculations also suggest an interpretation of the spectral blue shifts: With the 6-31G(d,p) basis set, the  $S_1 \leftarrow S_0$  transition of 2-pyridone is dominantly (93%) an excitation from the  $\pi$  HOMO to the  $\pi^*$  LUMO, with a minor excitation from the  $\pi$  HOMO-2 to the  $\pi^*$  LUMO+2. The former excitation involves a transfer of  $\pi$ -electron density from the  $2p_z$  orbital of the carbonyl oxygen atom to the ring  $\pi$ -electron system. This loss of electron density from the carbonyl group leads to a weakening of the C=O...H-N hydrogen bond upon electronic excitation. CIS calculations with diffuse basis sets [6-31+G(d,p) and 6-31++G(d,p)] predict that the  $S_1$  configuration state function remains dominated by one or two  $\pi^*$  orbitals; however, there are small contributions from low-lying  $\sigma^*$  orbitals. In contrast to our previous interpretation,<sup>9</sup> we now conclude that the main effect is due to the  $\pi\pi^*$  excitation and that mixing with low-lying Rydberg-type  $\pi\sigma^*$  excitations plays a minor role.

**C. Watson-Crick and Wobble Isomers of 2PY·Uracil and 2PY·Thymine.** The excellent correlation between the CIS/6-31G(d,p) calculated and observed spectral shifts in Figure 5 stimulated us to search for the spectra of the Watson-Crick and wobble isomers of 2PY·uracil and 2PY·thymine. On the basis of the calculated  $D_0$  values in Table 1, these isomers are expected to be present at low abundance. From the CIS/6-31G(d,p) calculated spectral shifts and with the scale factor determined from Figure 5, we estimate the electronic origins of the Watson-Crick and wobble isomers of 2PY·U to lie at 30 573 cm<sup>-1</sup> (U2) and 30 555 cm<sup>-1</sup> (U3) and those of 2PY·T at 30 552 (T2) and 30 552 cm<sup>-1</sup> (T3), respectively. Figure 6 shows the spectral regions of the two-color R2PI spectra of 2PY·U and 2PY·T about 400 cm<sup>-1</sup> below the intense  $0_0^0$  bands of the sugar-edge isomers U1 and T1. Two weak and close-lying band systems are indeed observed: For 2PY·U two origins are observed at 30 575.8 cm<sup>-1</sup> and 30 564.6 cm<sup>-1</sup>, within 3 and 10

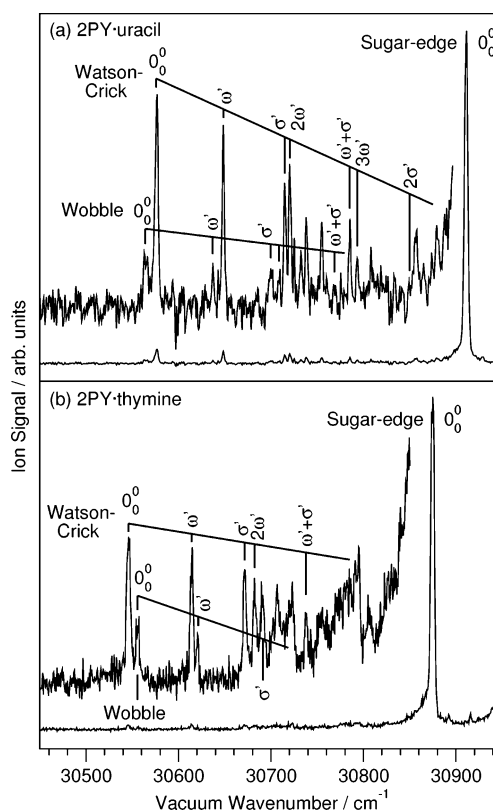


**Figure 6.** R2PI spectra of the Watson-Crick, wobble and sugar-edge isomers of 2PY·uracil (Watson-Crick  $0_0^0$  at 30 575.8, wobble  $0_0^0$  at 30 564.6 cm<sup>-1</sup>) and 2PY·thymine (Watson-Crick  $0_0^0$  at 30 545.5 cm<sup>-1</sup>, wobble  $0_0^0$  at 30 555.6 cm<sup>-1</sup>). The insets are magnified 10 times.

**TABLE 4: Experimental  $S_1$  State Vibrational Frequencies (in cm<sup>-1</sup>) of the Watson-Crick and Wobble Isomers of 2-Pyridone·Uracil and 2-Pyridone·Thymine**

	2-pyridone·uracil		2-pyridone·thymine	
	Watson-Crick (U2)	wobble (U3)	Watson-Crick (T2)	wobble (U3)
$0_0^0 (S_1 \leftarrow S_0)$	30575.8	30 564.6	30545.5	30 555.6
$\omega'$	72.5	72.5	68.9	64.9
$\sigma'$	139.3	135.6	126.3	134.8
$2\omega'$	144.6	144.2	137.2	
$\omega' + \sigma'$	209.3	203.4	192.5	

cm<sup>-1</sup> of the calculated values. For 2PY·T, two origins are observed at 30 545.5 cm<sup>-1</sup> and 30 555.6 cm<sup>-1</sup>, within 7 and 5 cm<sup>-1</sup> of the calculated values.

The measured low-frequency intermolecular vibrational excitations of the U2, U3, T2 and T3 isomers are assigned in analogy to the dimers. The assignments and frequencies are listed in Table 4 and are in good agreement with the CIS calculated frequencies, given in Table 2.

With the PW91/6-311++G(d,p) vibrational frequencies and rotational constants, the free energy of isomerization for 2PY·uracil at 513 K is calculated to be  $\Delta G_{\text{isom}}^0 = +3.30$  kcal/mol for the sugar-edge(U1)  $\rightarrow$  Watson-Crick(U2) and  $\Delta G_{\text{isom}}^0 = +4.51$  kcal/mol for the sugar-edge(U1)  $\rightarrow$  wobble(U3) isomerization; see also Table 1. These free energy changes correspond to abundances of 3.9% for the Watson-Crick and 1.2% for the wobble isomer in the molecular-beam source at 513 K. The measured electronic origin intensities are  $4.2 \pm 0.25\%$  (U2) and  $1.2 \pm 0.25\%$  (U3) of the U1 electronic origin; see Figure 6. The RMS background noise level is taken as the uncertainty. The calculated and measured isomer ratios are seen to agree within the experimental error.

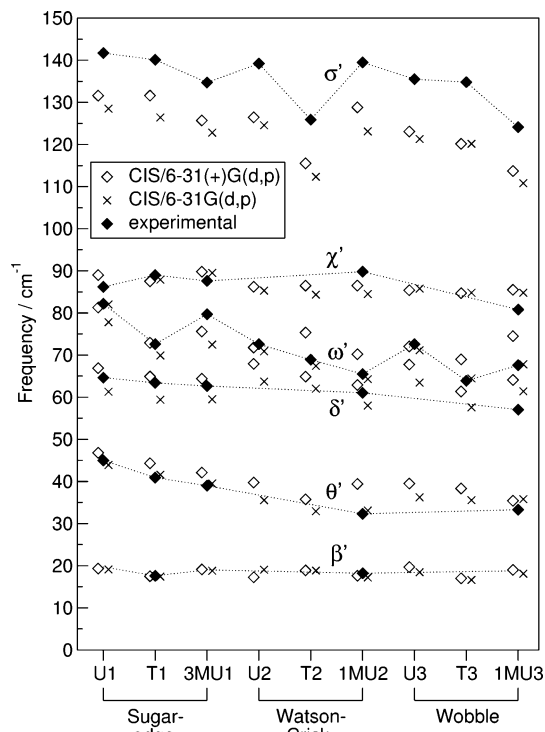


**Figure 7.** Comparison of experimental and CIS/6-31G(d,p) and 6-31-(+)-G(d,p) calculated intermolecular  $S_1$  state frequencies.

For the 2-pyridone·thymine isomerization, the calculated isomerization free energy at 483 K is  $\Delta G_{\text{isom}}^\ominus = +3.59$  kcal/mol for the sugar-edge(T1)  $\rightarrow$  Watson-Crick(T2) isomerization. This leads to a calculated abundance of 2.4%, in acceptable agreement with the measured abundance of  $1.7 \pm 0.25\%$ . Alternatively, we can convert the observed concentration ratio at 483 K to an experimental isomerization free energy  $\Delta G_{\text{isom}}^\ominus = 4.1 \pm 0.3$  kcal/mol. For the sugar-edge(T1)  $\rightarrow$  wobble(T3) isomerization we calculate  $\Delta G_{\text{isom}}^\ominus = +4.37$  kcal/mol, leading to a predicted abundance of 1.0% for T3. This is in good agreement with the measured concentration ratio of  $0.7 \pm 0.25\%$ . The observed isomer ratio yields an experimental  $\Delta G_{\text{isom}}^\ominus = 4.8 \pm 0.5$  kcal/mol.

The good agreement of the calculated and experimental isomer ratios, both in this section and for 2PY·1MU in section IV.A, support the previous assumption that the isomer ratios are established within the molecular-beam source or early in the high-temperature, high-pressure zone of the expansion. Any later modification induced by the jet expansion would lower the concentrations of the less stable Watson-Crick and wobble isomers, which would increase the apparent experimental  $\Delta G_{\text{isom}}^\ominus$ . Hence, the values given above should be regarded as upper limits for  $\Delta G_{\text{isom}}^\ominus$ .

**D. Intermolecular Vibrations.** The experimentally observed intermolecular vibrational frequencies of the nine observed isomers of the four different 2PY·(methyl)uracil dimers are compared in Figure 7 to the CIS/6-31G(d,p) and CIS/6-31(+)-G(d,p) calculated frequencies. The respective sugar-edge, Watson-Crick and wobble isomers are grouped together; each group follows the sequence uracil-thymine-methyluracil. Several interesting trends and features are apparent:

(i) In general, the agreement of the observed and calculated frequencies is very good, with the exception of the  $\sigma'$  stretch vibrations. However, the latter frequencies are *uniformly* too low by 10–14  $\text{cm}^{-1}$  or 7–10%. This implies that the CIS

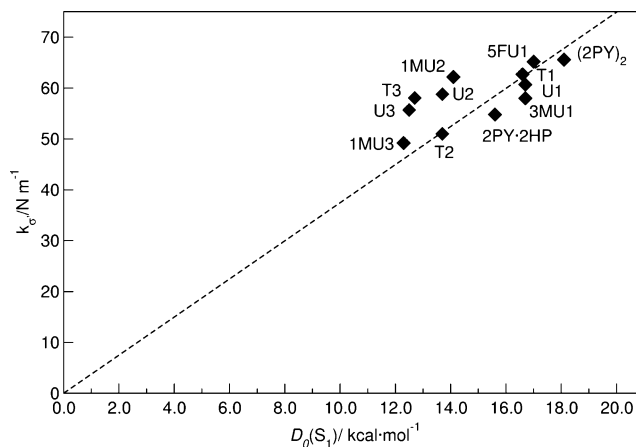


**Figure 8.**  $S_1$  state experimental pseudo-diatomic harmonic stretching force constants  $k_{\sigma'}$  of the 2PY·X dimers vs the excited-state dissociation energy  $D_0(S_1)$ .

method underestimates the curvature of the PES along the stretching coordinates but does so in a systematic way. The extension of the basis set by the diffuse orbitals on the H-bonding hydrogen atoms increases the frequency by 2–5  $\text{cm}^{-1}$ .

(ii) The  $\theta'$  propeller twist and  $\delta'$  stagger vibrational frequencies show a smooth decrease on going from left to right, i.e., from the sugar-edge to the wobble isomers.

(iii) The out-of-plane buckle vibration  $\beta'$  and the in-plane shear  $\chi'$  modes show very little dependence on either the isomer or degree of methylation, in both theory and experiment.

(iv) The  $\omega'$  opening frequencies generally decrease on going from left to right. However, for the sugar-edge and wobble isomers, the frequency varies rather erratically depending on whether the methyl group is at the 1-, 3- or 5-position. For the stretching frequencies, the effect is similar but typically has the opposite sign, i.e., when  $\omega'$  is unusually low,  $\sigma'$  is high. This indicates that the frequency changes are due to coupling between these two in-plane modes.

From the stretching frequencies  $\sigma'$ , one can deduce the  $S_1$  state H-bond stretching force constants  $k_{\sigma'}$  using the pseudo-diatomic harmonic oscillator model.<sup>9,26,33,38</sup> The reduced mass  $\mu$  for the dimers of 2PY involving the methyluracils is  $\mu = 54.21$   $u$ . The force constants (in N/m) are then calculated to be  $k_{\sigma'} = 58.0$  for 3MU1, 62.2 for 1MU2, 49.2 for 1MU3, 58.8 for U2, 55.7 for U3, 51.0 for T2 and 58.1 for T3. In Figure 8 we plot  $k_{\sigma'}$  vs the excited-state dissociation energy  $D_0(S_1)$ , including the previously determined stretching force constants for U1, T1 and 5FU.<sup>9</sup> Although the  $D_0(S_1)$  lies within 0.5 kcal/mol for all isomers bound through the same site, their force constants disperse over  $\approx 8$  N/m for the four sugar-edge isomers,  $\approx 11$  N/m for the three Watson-Crick dimers and  $\approx 9$  N/m for the three wobble dimers. These differences show that the stretching vibrations cannot be simply mapped onto pseudo-one-dimensional vibrational motions. Although for the three uracil isomers there is a monotonic trend of force constant as a function of dissociation energy, for 1-, 3- and 5-methyluracil, the derived force constants do not change systematically as a function of  $D_0$ . Obviously, the methylation has a considerable effect on the mass distribution of the uracil moiety and hence on the stretching vibrational eigenvectors and frequencies, which results in unsystematic changes of the pseudo-diatomic force constants.

## V. Conclusions

In this work we have probed the sugar-edge, Watson-Crick and wobble hydrogen-bonding sites of uracil and 1-, 3-, and



5-methyluracil (thymine) using 2-pyridone as a probe chromophore. Complexation of 2PY to 3-methyluracil selectively probes the sugar-edge binding site of uracil, because no other pairing is possible. The R2PI spectrum of 2PY·3-methyluracil exhibits the same spectral blue shift and Franck–Condon profile overall shape as the corresponding R2PI spectra of 2PY·uracil and 2PY·thymine; the effects of the methyl group turn out to be minor. H-bonding of 2PY to 1-methyluracil leads to both the Watson–Crick and wobble isomers; both structures are biologically relevant. The two R2PI spectra are separated by UV–UV hole-burning techniques. Comparison of R2PI and hole-burning spectra with CIS calculated excited-state frequencies allows an unequivocal assignment of the isomers.

The excited-state geometries, energies and vibrational frequencies of all the dimers were calculated using the CI-singles method with different basis sets. The adiabatic transition energies and spectral shifts relative to bare 2-pyridone were also calculated. The experimental spectral shifts of all 2PY·X complexes are to the blue, corresponding to a decrease of the H-bond dissociation energy by 2–3 kcal/mol. This behavior is very unusual for a  $\pi\pi^*$  transition. It can be rationalized on the basis of the CIS calculations, which indicate that  $S_1 \leftarrow S_0$  electronic excitation of 2PY transfers electron density from its H-bonded carbonyl O atom toward the ring system. This electron flow weakens the (2PY)C=O···H–N hydrogen bond and lowers the excited-state dissociation energy, inducing a spectral blue shift.

For the nine isomers of 2PY·U, 2PY·U, 2PY·1-methyluracil and 2PY·3-methyluracil we have determined 35 of the 54 intermolecular vibrational frequencies in the  $S_1$  state. The observed frequencies are generally in excellent agreement with those calculated by the CIS method with the 6-31G(d,p) and CIS/6-31(+)-G(d,p) basis sets, with the exception of the stretching frequencies. These are systematically too low by  $\approx 10\%$  for the 6-31G(d,p) and by 7% for the 6-31G(+)(d,p) basis set. The different H-bond topologies of the (methyl)uracil complexes give rise to vibrational frequency patterns that are characteristic for individual isomers.

The CIS/6-31G(d,p) calculated spectral shifts correlate very well with the experimental values for the 2PY dimers with uracil, 1-, 3-, 5-methyluracil, 5-fluorouracil, 2-hydroxypyridine, and H<sub>2</sub>O. On the basis of this correlation, the predicted spectral shifts of the Watson–Crick and wobble isomers of 2PY·uracil and 2PY·thymine allowed us to identify the weak spectra of these isomers, which are present in the gas phase at concentrations of 1–4%. The relative isomer abundances between the sugar-edge, Watson–Crick and wobble isomers of 2PY·uracil and 2PY·thymine and between the Watson–Crick and wobble isomers of 2PY·1-methyluracil are in good agreement with the isomerization free energies calculated by the PW91 DFT method. This allows us to determine the relative dissociation energies of the Watson–Crick and wobble isomers relative to the sugar-edge isomers.

**Acknowledgment.** This work was supported by the Schweiz. Nationalfonds (proj. no. 2000-68081.02 and 200020-105490)

and by the Centro Svizzero di Calcolo Scientifico (CSCS) in Manno, Switzerland.

## References and Notes

- Weinkauff, R.; Schermann, J.-P.; de Vries, M.; Kleinermaans, K. *Eur. Phys. J. D* **2002**, *20*, 309.
- Périsquet, V.; Moreau, A.; Carles, S.; Schermann, J. P.; Desfrancois, C. *J. Electron. Spectrosc. Relat. Phenom.* **2000**, *106*, 141.
- Kratochvil, M.; Engkvist, O.; Šponer, J.; Jungwirth, P.; Hobza, P. *J. Phys. Chem. A* **1998**, *102*, 6921.
- Leininger, M. L.; Nielsen, I. M. B.; Colvin, M. E.; Janssen, C. L. *J. Phys. Chem. A* **2002**, *106*, 3850.
- Kratochvil, M.; Engkvist, O.; Vacek, J.; Jungwirth, P.; Hobza, P. *Phys. Chem. Chem. Phys.* **2000**, *2*, 2419.
- Brady, B. B.; Peteanu, L. A.; Levy, D. H. *Chem. Phys. Lett.* **1988**, *147*, 538.
- Onidas, D.; Markovitsi, D.; Marguet, S.; Sharonov, A.; Gustavsson, T. *J. Phys. Chem. B* **2002**, *106*, 11367.
- Gustavsson, T.; Sharonov, A.; Markovitsi, D. *Chem. Phys. Lett.* **2002**, *351*, 195.
- Müller, A.; Leutwyler, S. *J. Phys. Chem. A* **2004**, *108*, 6156.
- Saenger, W. *Principles of Nucleic Acid Structures*; Springer, Berlin: 1984.
- Jeffrey, G. A.; Saenger, W. *Hydrogen Bonding in Biological Structures*; Springer, Berlin: 1991.
- Cech, T. R.; Damberger, S. H.; Gutell, R. R. *Nat. Struct. Biol.* **1994**, *1*, 273.
- Grüne, M.; Fürste, J. P.; Klusmann, S.; Erdmann, V. A.; Brown, L. R. *Nucl. Acids Res.* **1996**, *24*, 2592.
- Leontis, N. B.; Stombaugh, J.; Westhof, E. *Nucleic Acids Res.* **2002**, *30*, 3479.
- Stewart, R. *Acta Crystallogr.* **1967**, *23*, 1102.
- Nir, E.; Müller, M.; Grace, L. I.; de Vries, M. S. *Chem. Phys. Lett.* **2002**, *355*, 59.
- Plützer, C.; Hünig, I.; Kleinermaans, K. *Phys. Chem. Chem. Phys.* **2003**, *4*, 4877.
- Plützer, C.; Hünig, I.; Kleinermaans, K.; Nir, E.; de Vries, M. *Chem. Phys. Chem.* **2003**, *4*, 838.
- Müller, A.; Losada, M.; Leutwyler, S. *J. Phys. Chem. A* **2004**, *108*, 157.
- Hobza, P.; Šponer, J. *J. Am. Chem. Soc.* **2002**, *124*, 11802.
- Boys, S. F.; Bernardi, F. *Mol. Phys.* **1970**, *19*, 553.
- Bukowski, R.; Jeziorski, B.; Szalewicz, K. *J. Chem. Phys.* **1996**, *104*, 3306.
- Tanner, C.; Manca, C.; Leutwyler, S. *Chimia* **2004**, *58*, 234.
- Manca, C.; Tanner, C.; Leutwyler, S. *Chimia* **2004**, *58*, 287.
- Manca, C.; Tanner, C.; Coussan, S.; Bach, A.; Leutwyler, S. *J. Chem. Phys.* **2004**, *121*, 2578.
- Müller, A.; Talbot, F.; Leutwyler, S. *J. Chem. Phys.* **2000**, *112*, 3717.
- Müller, A.; Talbot, F.; Leutwyler, S. *J. Chem. Phys.* **2002**, *116*, 2836.
- Held, A.; Champagne, B. B.; Pratt, D. *J. Chem. Phys.* **1991**, *95*, 8732.
- Nimlos, M. R.; Kelley, D. F.; Bernstein, E. R. *J. Phys. Chem.* **1989**, *93*, 643.
- Held, A.; Pratt, D. *J. Am. Chem. Soc.* **1990**, *112*, 8629.
- Held, A.; Pratt, D. *J. Chem. Phys.* **1992**, *96*, 4869.
- Borst, D. R.; Roscioli, J. R.; Pratt, D. W.; Florio, G. M.; Zwier, T. S.; Müller, A.; Leutwyler, S. *Chem. Phys.* **2002**, *283*, 341.
- Müller, A.; Talbot, F.; Leutwyler, S. *J. Chem. Phys.* **2001**, *115*, 5192.
- Held, A.; Pratt, D. *J. Am. Chem. Soc.* **1993**, *115*, 9708.
- Turro, N. J. *Modern Molecular Photochemistry*; Benjamin: Menlo Park, 1978.
- Sobolewski, A. L.; Domcke, W. *Phys. Chem. Chem. Phys.* **1999**, *1*, 3065.
- Sobolewski, A. L.; Domcke, W. *J. Phys. Chem. A* **2001**, *105*, 9275.
- Müller, A.; Talbot, F.; Leutwyler, S. *J. Am. Chem. Soc.* **2002**, *124*, 14486.